行政院國家科學委員會補助專題研究計畫成果報告

利用離子電透入輸藥法促進 nalbuphine 前驅藥經皮吸收之研究
Transdermal Delivery of Novel Nalbuphine Prodrugs Using Iontophoresis

計畫類別：☑個別型計畫　□整合型計畫

計畫編號：NSC 89-2314-B-041-001

執行期間：　88 年 8 月 1 日至 89 年 7 月 31 日

計畫主持人：主持人：宋國峻

本成果報告包括以下應繳交之附件：

□赴國外出差或研習心得報告一份

□赴大陸地區出差或研習心得報告一份

□出席國際學術會議心得報告及發表之論文各一份

□國際合作研究計畫國外研究報告書一份

執行單位：嘉南藥理科技大學藥學系

中　華　民　國　89　年　10　月　25　日

行政院國家科學委員會專題研究計畫成果報告

利用離子電透入輸藥法促進nalbuphine前驅藥經皮吸收之研究

Transdermal Delivery of Novel Nalbuphine Prodrugs Using Iontophoresis

計畫編號：NSC 89-2314-B-041-001

執行期限：88年8月1日至89年7月31日

主持人：宋國峻　嘉南藥理科技大學藥學系

I. Abstract

The in vitro permeation of nalbuphine (NA) and its prodrugs across skins were investigated in the present study to assess the effects of prodrug hydrophilicity-lipophilicity on the passive as well as iontophoretic permeation.

Keywords: nalbuphine; nalbuphine prodrug; transdermal delivery; iontophoresis

II. Introduction

In the present study, two major goals are to be achieved. The first goal is to assess the transdermal characteristics of NA and its prodrugs under passive diffusion and iontophoresis in order to demonstrate the influence of drug hydrophilicity-lipophilicity on skin permeation characteristics under various driving forces. The second goal is to utilize various skin membranes as permeation barriers, including hairless mouse skin, stratum corneum (SC)-stripped skin, delipid skin, furry Wistar rat skin and human skin, to explore the transdermal mechanisms of NA and its prodrug under passive diffusion as well as iontophoresis. These studies may help to elucidate the different transdermal mechanisms involved in the transdermal delivery of NA and its prodrugs under passive diffusion and iontophoresis.

III. Results and Discussion

Passive Permeation of NA and Its Prodrugs

Table I shows the n-octanol/water partition coefficients of NA and its prodrugs. The chemical modifications of NA indeed result in the change of its physicochemical properties, with higher partition coefficients for prodrugs with longer ester side chains (Table I). Figure 1 shows the cumulative amounts of NA (in nmole/cm^2) in the receptor site as a function of time profiles for the passive permeation of NA and its prodrugs. The apparent steady-state fluxes (Jss) and permeability coefficients (Kp) obtained from the profiles were summarized in Table I. Both Figure 1 and Table I show that the permeability coefficients of those drugs increased with the drug lipophilicity, with the order of NAD>NAE>NAP>NA.

Iontophoretic Permeation of NA and Its Prodrugs

Figure 2 shows the amount of drug permeated (in nmole/cm^2) versus time profiles for NA and its prodrugs in pH 4 buffer under iontophoresis with a constant current of 0.3 mA/cm^2. The apparent steady-state fluxes (J_{ss}) and permeability coefficients (K_p) obtained from the profiles were also listed in Table I. The data in Table I demonstrate that both the fluxes and permeability coefficients of NA and its prodrugs increased significantly after application of external electric field. The trend of permeability coefficients for the four analogues under iontophoresis were different from that under passive permeation, with the order of NAD>NAE>NA>NAP. While comparing the permeability coefficients of the drugs under iontophoresis to those under passive diffusion, a series of enhancement ratios (ER) for the four analogues were obtained (Table I). The

ER for NA was highest (107.36), and decreased as the drug lipophilicity increased, with the ER of 2.31 for NAD. The results suggest that the application of iontophoresis has more pronounced enhancement effects on the permeation of more hydrophilic drug.

Passive Permeation of NA and NAP across Various Skins

Table II shows the fluxes and permeability coefficients of NA and NAP across various skins via passive diffusion. Except for the delipid skin, NAP had higher permeability coefficients than NA in all the skin membranes studied. The data in Table II also demonstrate that the permeability coefficients of NA and NAP diffused across SC-stripped skins were 40.79 and 9.18 fold higher than those across intact skin, suggesting that permeation through the SC layer was the rate-limiting process for the passive permeation of NA and NAP across the skins. The higher enhancement effect in permeability coefficients for NA relative to NAP after removal of SC indicating that the SC layer had more pronounced barrier effect on the more hydrophilic drug.

Table II also demonstrates that the permeability coefficient of NA across furry Wistar rat skin was 3-times higher than that of NA across hairless mouse skin; whereas no significant difference in permeability coefficient was observed for NAP permeated through Wistar rat and hairless mouse skins. The observation indicates that the transappendageal routes constitute the more important permeation pathways for the more hydrophilic drug. Furthermore, the permeability coefficient of NA across human skin was comparable to that across hairless mouse skin in the present study, suggesting the feasibility of using hairless mouse skin to represent human skin as the barrier membrane in the in vitro passive permeation experiments of NA and its prodrugs.

Iontophoretic Permeation of NA and NAP across Various Skins

Table III shows the permeability coefficients of NA across various skins under iontophoresis. No significant difference (t-test, $p > 0.05$) was observed between the permeability coefficients of NA across intact skin and SC-stripped skin of hairless mouse; furthermore, similar permeation coefficients (t test, $p>0.05$) were also obtained between the permeation of NA across intact skin and delipid skins. Those data indicate that the SC layer was not a rate-limiting barrier for the transport of NA across the skin under iontophoresis. That is, the rate-limiting characteristics of SC layer in the passive transport of NA could be overcome by application of iontophoresis. Since the magnitude of permeability coefficient for NA across hairless mouse skin via passive diffusion (K_o) is negligible comparing to the K_{total} (Table II and III), the overall permeation enhancement of NA under iontophoresis is due primarily to the permeability arised from the electrochemical potential gradient ($K_{\triangle v}$) and the increase in skin permeability induced by the field (K_s).

For the permeation of NAP under iontophoresis, however, the permeability coefficient for NAP across the SC-stripped skin was significantly higher than that across intact skin (Table III). The data again indicate that the SC layer retarded the iontophoretic permeation of NAP and showed a rate-limiting characteristic for the permeation of NAP across skins. Moreover, the permeability coefficient of NAP across delipid skin was comparable to that across SC-stripped skin, suggesting the intercellular lipid matrix but not intracellular corneocytes was the major route for the permeation of NAP across SC layer during iontophoresis. The above results were consistent with previous publications that iontophoresis may increase the access of ions to the intercellular lipid lamellae. By comparing the permeability coefficients of NA and NAP through various skins under iontophoresis, the results clearly demonstrate that different rate-determined processes involved in the iontophoretic delivery of NA and NAP across the skins.

Table III shows the permeability coefficients and ER values for drugs permeated through the Wistar rat skin under iontophoresis. By comparing the permeability coefficients of NA as well as NAP through the

hairless mouse and Wistar rat skin, the data demonstrate that the appendageal pathways (i.e. hair follicles and sweat glands) are the more important routes for the transdermal iontophoretic delivery of NA than NAP. Table III also shows that NA had higher iontophoretic ER across furry Wistar rat skin than that of NAP (45.17 versus 9.21). Those data suggest that a significant portion of NA may permeate through skin via the appendageal pathways under iontophoresis, whereas NAP permeated predominantly through the lipid matrix. The results are similar to the previous findings that the appendageal routes constitute important pathways for NA under passive diffusion. Table III also shows that the permeability coefficients of NA and NAP across human skin under iontophoresis was much lower as compared with those across hairless mouse and Wistar rat skins. The phenomenon can be attributed to that the full-thickness human skin was used in the in vitro permeation experiment and the lack of natural blood supply may underpredict iontophoretic delivery due to sequestration of the permeant . Another explanation is that the human skin has 1/10 ~ 1/100 less hair follicles than hairless mouse skin, resulting in the significant reduction of permeability across human skin under iontophoresis.

IV. References

1. E. Varghese and R. K. Khar. J. Control. Release 38 (1996) 21-27.
2. J. E. Riviere and M. C. Heit. Pharm. Res. 14 (1997) 687-697.
3. S. Del Terzo, C. R. Behl and R. A. Nash. Pharm. Res 6 (1989) 85-90.
4. L. L. Wearley, K. Tojo and Y. W. Chien. J. Pharm. Sci. 79 (1990) 992-998.
5. J. Hirvonen, Y. N. Kalia and R. H. Guy. Nature Biotechnology 14 (1996) 1710-1713.
6. K. Kontturi and L. Murtomaki. J. Control. Release 41 (1996)177-185.

V. Comments

This NSC supported project has been thoroughly studied under the guidance of the principle investigator. The final results of this research have been written in a manuscript and this manuscript has been accepted by the Journal of Controlled Release.

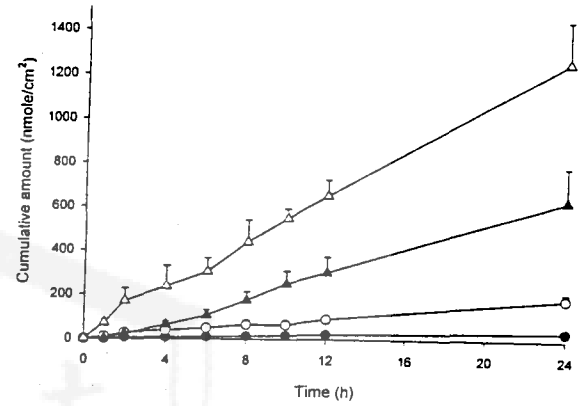

Fig. 1. Cumulative amount of drug permeated per unit area (nmol/cm^2) versus time profiles under passive diffusion: nalbuphine (●), nalbuphine pivalate (○), nalbuphine enanthate (▲) and nalbuphine decanoate (△). All data represent the means of three experiments±S.D.

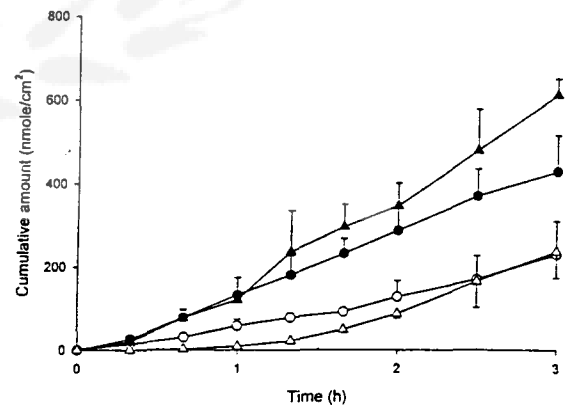

Fig. 2. Cumulative amount of drug permeated per unit area (nmol/cm^2) versus time profiles under iontophoresis: nalbuphine (●), nalbuphine pivalate (○), nalbuphine enanthate (▲) and nalbuphine decanoate (△). All data represent the means of three experiments±S.D.

Table 1
Physicochemical properties and in vitro permeation data of nalbuphine and its prodrugs

Drug		MW[a] (Da)	log P[b]	Flux (nmol/cm^2/h)	K_p[c] ($\times 10^{-3}$ cm/h)	ER[d]
Nalbuphine	Passive	357.46	0.17	1.40±0.28	0.50±0.10	–
	Iontophoresis			150.30±31.34	73.70±1.20	103.36
Nalbuphine pivalate	Passive	441.59	1.42	7.22±1.86	2.58±0.66	–
	Iontophoresis			79.16±25.49	28.30±9.11	10.96
Nalbuphine enanthate	Passive	469.62	1.94	27.19±6.53	12.77±3.07	–
	Iontophoresis			222.78±20.05	104.63±9.42	8.19
Nalbuphine decanoate	Passive	511.70	3.30	51.58±9.80	53.95±10.25	–
	Iontophoresis			19.02±34.52	124.48±36.11	2.31

[a] MW = Molecular weight.
[b] P = n-Octanol–water partition coefficient.
[c] K_p = Permeability coefficient = flux/concentration of drug in the donor vehicle.
[d] ER = Enhancement ratio = iontophoretic flux/passive flux. Each value represents the mean±S.D. (n = 3).

Table 2
The data for in vitro passive permeation of nalbuphine and nalbuphine pivalate across various skins

Drug	Skin types	Flux (nmol/cm^2/h)	K_p[a] ($\times 10^{-3}$ cm/h)
Nalbuphine	Hairless mouse	1.40±0.28	0.50±0.10
	SC-stripped	57.11±15.84	20.42±3.67
	Delipid	54.62±15.84	19.52±5.66
	Wistar rat	4.60±1.10	1.64±0.39
	Human	1.68±0.34	0.60±0.12
Nalbuphine pivalate	Hairless mouse	7.22±1.86	2.58±0.66
	SC-stripped	70.60±4.04	25.24±1.44
	Delipid	57.58±16.18	20.59±5.78
	Wistar rat	8.75±2.47	3.13±0.88
	Human	2.94±1.32	1.05±0.47

[a] K_p = Permeability coefficient = flux/concentration of drug in donor vehicle. Each value represents the mean±S.D. (n = 3).

Table 3
The data for in vitro iontophoretic permeation of nalbuphine and nalbuphine pivalate across various skins

Drug	Skin types	Flux (nmol/cm^2/h)	K_p[a] ($\times 10^{-3}$ cm/h)	ER[b]
Nalbuphine	Hairless mouse	150.30±31.34	53.70±11.20	107.36
	SC-stripped	186.77±25.59	66.99±9.14	3.27
	Delipid	130.10±28.97	46.48±10.35	2.38
	Wistar rat	207.79±67.06	74.24±23.96	45.17
	Human	8.37±2.21	2.99±0.79	4.98
Nalbuphine pivalate	Hairless mouse	79.16±25.49	28.30±9.11	10.96
	SC-stripped	138.57±28.75	49.54±10.28	1.96
	Delipid	125.76±16.10	44.96±5.76	2.51
	Wistar rat	80.61±20.68	28.82±7.39	9.21
	Human	38.06±16.29	13.61±5.82	12.95

[a] K_p = Permeability coefficient = flux/concentration of drug in donor vehicle.
[b] ER = Enhancement ratio = iontophoretic flux/Passive flux. Each value represents the mean±S.D. (n = 3).